International Journal of Pharmaceutics, 67 (1991) 231–246
Elsevier Science Publishers B.V. (Biomedical Division)
ADONIS 037851739100101V

IJP 02224

Tablet bond. II. Experimental check of model

E.N. Hiestand and D.P. Smith

The Upjohn Co., Kalamazoo, MI 49001 (U.S.A.)

(Received 10 August 1989)
(Modified version received 2 March 1990)
(Accepted 21 June 1990)

Key words: Compact; Particle; Tensile strength; Hardness; Viscoelasticity; Surface energy; Elastic modulus; Strain index; Radius of curvature; Brittle separation; Ductile extension

Summary

The modeling of tablet bond formation requires two mechanisms. The theory was presented in Part I (Hiestand, E.N., *Int. J. Pharm.*, 67 (1991) 217–229). The ductile mechanism if it operates occurs at lower compression forces. The brittle mechanism operates at higher compression forces and may be the only mechanism acting for some materials. Sorbitol is used to illustrate the two mechanism case and phenacetin illustrates the one mechanism case. Cellulose, lactose, and acetaminophen data tend to support the models; but are complicated by particle fracture during compression or mixed regions where both mechanisms may be occurring at different particles within the compact. However, none of the experimental data led to a rejection of these models for tablet bond formation.

Introduction

Two models describing the mechanisms of tablet bond were developed in part I (Hiestand, 1991); the equations are variations of Johnson's approach (Johnson, 1976). These models emphasize the role of the mechanical properties of the powder particles. Two basic equations were developed. Both assumed that the compression pressure produced true contact areas between particles as a result of plastic deformation; and the forces of attraction were those of the surface energy. Since the surface energy of solids covers a small range, mostly in the 30–70 dyn/cm. interval, the differences of bonding characteristics must be due principally to differences of mechanical properties. Those properties, including the surface energy, will determine the processes during the separation of contacting surfaces caused by the unloading of the internal elastic energy. Since tensile loads are just an extension of the unloading, the same mechanisms continue and determine the tensile strength.

Correspondence: E.N. Hiestand, 11, 378 East G Avenue, Galesburg, MI 49053, U.S.A.

Tensile Strength; Tablet Bond

One of the models for tablet bond assumed that stress concentrations at the edge of the contact areas between two particles would best be described as equivalent to crack propagation, fracture mechanics. This will be referred to as the *brittle mechanism*. Viscoelastic effects were included by assuming that the mechanical property values acting at a given time or at a given strain rate could be used in conventional equations (Wil-

liams, 1980). That tensile strength model led to Eqn 1.

$$\sigma_{Tv} = Nf''_{am} = -\left(\frac{2\epsilon_t H_0 \Delta\gamma}{\epsilon_\infty \epsilon_0 H_t}\right)\left(\frac{N\sigma_c}{\pi H_c}\right)^{1/2} \quad (1)$$

where σ_{Tv} is the tensile strength of the compact of a viscoelastic material for the brittle mechanism, σ_c is the pressure used to compress the compact, f''_{am} is the mean tensile strength of a single contact point, N is the number of contact points in a fracture unit cross section, H is the indentation hardness, ϵ is the strain index, H/E', where E is Young's modulus and υ is Poisson's ratio when

$$\frac{1}{E'} = \frac{1-\upsilon_1^2}{E_1} + \frac{1-\upsilon_2^2}{E_2}$$

The subscripts refer to the particles, respectively. $\Delta\gamma$ is the change of surface energy between contact and separation. Subscripts 0, t, c, and ∞ refer to the time frame or rate of the specific event: 0 designates an instantaneous event, t designates the rate associated with the elastic recovery, c designates the rate associated with the dwell time of the compression pressure, and ∞ designates the totally relaxed condition.

The second model assumed plastic deformation of the contact region, isthmus formation, occurred during the unloading of the elastic energy. Ductile extension, i.e. isthmus formation, had been proposed as a mechanism for strong tablet bond (Hiestand and Smith, 1984). This process would extend to tensile loading. Criteria were established for the conditions that would result in ductile extension. The model gave Eqn 2 for the tensile strength of a compact when this *ductile mechanism* is controlling. (Note that the brittle and ductile mechanism terminology used herein refer to *decompression*. These terms sometimes are used for compression, brittle being the fracture of particles and ductile the plastic deformation of the particles as a response to the compression stress.)

$$\sigma_{Td} = Nf_{adm} = -\left(\frac{64N}{\pi H_t^3}\right)\left(\frac{H_0 \Delta\gamma}{\epsilon_0}\right)^2 \quad (2)$$

where σ_{Td} is the tensile strength of the compact for the ductile mechanism and f_{adm} is the mean tensile strength at an individual contact region. For this equation, the viscoelastic effect was treated in a manner analogous to that of Eqn 1.

Application limitations of Eqns 1 and 2

Eqns 1 and 2 have limited application; they apply over a limited range of solid fractions. Within themselves, they do not indicate this range. The limitations are discussed below.

Both Eqns 1 and 2 assume that the tensile strength of the compact is the sum of the individual interparticle strengths. As used herein, tensile strength is defined as the fracture strength of the compact. This model would not predict the tensile strength if the compact underwent ductile extension instead of brittle fracture. Furthermore, this summation approach suggests that compact strength should exist as long as there is attraction between particles. However, compact tensile strength becomes essentially zero when uninhibited particle rearrangement becomes possible, i.e. when the shear strength becomes essentially zero. This happens when N has a finite but very small value, i.e. the compact tensile strength will go to zero before N becomes zero. (N is an average value; it may be finite when three-dimensional continuity is lost.) Also, the interparticle strength need not go to zero for the compact tensile strength to go to zero. When fitting plotted experimental tensile strength data, one obtains an intercept. Neither Eqn 1 nor 2 predicts this intercept. However, Eqns 1 and 2 should provide the slope of plots of tensile strength vs N.

Neither Eqn 1 nor 2 will predict whether the mechanism they describe acts at a given solid fraction. Criteria have been derived for doing this (Hiestand, 1991). Thus, the experimentalist must be aware of the limitations of the application of both equations.

A further complication arises because of the discontinuous nature of the calculated packing or contacts parameter, N'. (N' is the number of contacts in an area equal to r^2 and is less than the number of contacts per particle, $N' = Nr^2$.) N' is used instead of N in most of the discussion because it separates the particle size from the calcu-

lation. Rumpf's equation for N (Rumpf, 1962) is used below a solid fraction of 0.74. Also a coordination number of three is assumed in this range. This gives $N' = 9\rho_r/2\pi$ and is applicable when $N' \leqq 1.06$. Since tensile strengths with some materials have been measured for compacts with solid fraction below 0.4, it is questionable whether a constant coordination number of 3 should have been used in this low region. However, the experimental data, σ_T vs N', was sufficiently linear in this region to mask a need for such an adjustment. For $N' \geqq 1.06$, $N' = (1.71\rho_r + 0.067)/(2 - \rho_r)$ is used (Hiestand, 1991). The coordination number is assumed to increase linearly from 3 at $\rho_r = 0.74$ to 4 at $\rho_r = 1$.

Perhaps a more fundamental problem is how does one measure a strength that corresponds to the conditions described by the theory. The answer is elusive because compacts are Mohr bodies. Therefore, the experimental values obtained will depend on how the strength is measured. Direct tensile loading produces a very broad range of values. As discussed later, a reproducible method has been adopted. Only the slopes of tensile strength vs N' will be compared. No effort is made to calculate the absolute strength.

The 'contacts parameter', N'

Historically, plots of log σ_T vs ρ_r and of log σ_c vs ρ_r have been shown to be nearly linear over most of the range. This is not completely compatible with the expectation that plots of σ_T or σ_c vs N' should be linear. Fig. 1 is a plot of log N' vs ρ_r. Clearly, the plot deviates only modestly from

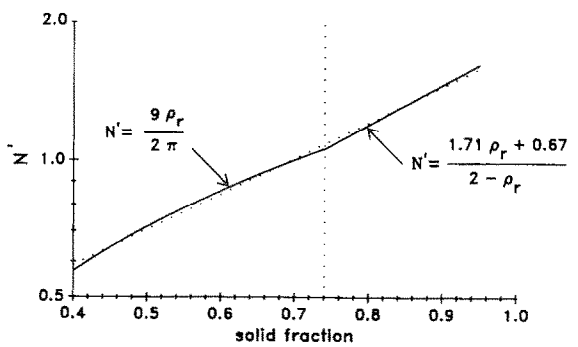

Fig. 1. Log N' vs ρ_r shows the least square line of data generated by calculating log N'; data obtained using the insert equations. The equations change at $\rho_r = 0.74$.

linearity; also, a transition is evident in the region where the method of calculating N' changes, at approximately $\rho_r = 0.74$. Thus, N' is more comparable to 10^{ρ_r} than to ρ_r. For many materials, both the σ_T vs N' and σ_c vs N' plots appear to break into two straight line portions. Apparently, the "scatter" of the data and the loss of sensitivity from using solid fraction mask this feature when using log σ_T vs ρ_r plots.

Separating Compact and Particle Properties

With N defined only in terms of solid fraction and particle size, it is possible to arrange terms so that the directly measured properties of the compacts correspond to the results calculated from the properties of the particles. The particle size is a particle property; and by removing it from N, i.e. using N', the particle size can be included with the particle properties. Eqn 1 can be written as in Eqn 3, where k_g has the dimensions of force per unit area and is a constant characteristic of the material. (Fracture of particles during compression would result in k_g not being a constant; k_g is inversely proportional to r^2.)

$$\frac{\sigma_{Tv}^2}{\sigma_c} = k_g N' - b \tag{3}$$

While the form of Eqn 3 is derived from Eqn 1, the constant, k_g, will be obtained from the graphical plots of the data. When the constant is calculated from the particle properties defined in Eqn 1, the subscript p will be used, i.e. k_p. The plots to obtain k_g do have an intercept, b, not obtained in the derivation of Eqn 1; but the first derivative is k_g, which should be equivalent to k_p.

Eqn 2 appears to be a different form and is written as in Eqn 4 with k_g' as the material constant. k_g' also has the dimensions of force per unit area.

$$-\sigma_{Td} = k_g' N' - b' \tag{4}$$

Again an intercept, b', is added arbitrarily to match the real data. b' is not predicted in Eqn 2. The slope of a plot of σ_T vs N' would be k_g'.

Again the subscript p, i.e. k'_p, is used for the equivalent constant calculated from the particle properties defined in Eqn 2. Note that in Eqn 2 the compression pressure would influence the tensile strength only as a result of changes in N.

The plots of σ_T^2/σ_c vs N', used to obtain k_g, sometimes have excessive 'scatter'. Much of this is due to combining the experimental error of the compression pressure with that of the square of the tensile strength. Also the experimental σ_c may include an intraparticle hydrostatic component that does not contribute to the formation of areas of true contact useable for bonding. The areas would be ineffective because that portion of the hydrostatic component that occurs within the particle does not produce shear stresses and plastic deformation of the particle. Areas of true contact developed by intraparticle hydrostatic components change neither a_c nor R. Therefore, intraparticle hydrostatic stresses do not change the bond strength for the brittle mechanism. The ductile bond strength is independent of a_m once a_d has been reached. Since this hydrostatic component cannot be removed from the experimental σ_c, it will contribute to the distortion of the plot of σ_T^2/σ_c vs N'. In the absence of a better alternative, the magnitude of graphical values for k'_g must be compared to the equivalent values derived from Eqn 2.

k_p and k'_p are defined in Eqns 5 and 6:

$$k_p = \left(\frac{2\epsilon_t H_0 \Delta\gamma}{\epsilon_0 \epsilon_\infty H_t r}\right)^2 \left(\frac{1}{\pi H_c}\right) \tag{5}$$

$$k'_p = \left(\frac{64}{\pi H_t^3}\right)\left(\frac{H_0 \Delta\gamma}{r\epsilon_0}\right)^2 \tag{6}$$

If $H_c = H_t$ then Eqn 7 may be obtained by combining Eqns 5 and 6.

$$k'_p = 16 k_p \left(\frac{\epsilon_\infty}{\epsilon_t}\right)^2 \tag{7}$$

It must be remembered that Eqn 3 describes a different bonding mechanism than does Eqn 4. Therefore, the two tensile strengths are not necessarily equal even for the unique value where the mechanism changes. Nevertheless, because k_g and k'_g are slopes, they may be substituted into Eqn 7 for the calculated slopes without encountering this problem. Thus, $\epsilon_t/\epsilon_\infty$ can be estimated from slopes obtained from compact data as shown in Eqn 8.

$$\frac{\epsilon_t}{\epsilon_\infty} = \left(\frac{16 k_g}{k'_g}\right)^{1/2} \tag{8}$$

Both mechanisms, ductile and brittle, cannot be acting simultaneously at a specific contact point. However, it is possible in a compact for both mechanisms to be operating simultaneously but at different contact points. Therefore, the graphical estimates of either constant may be slightly in error, i.e. data from a mixed region may be inadvertently included in determining the constant. Some arbitrary judgement may be necessary to eliminate data in this transition region. With both k values determined graphically and substituted into Eqn 8, an estimate of $\epsilon_t/\epsilon_\infty$ is obtained. This ratio for the compact should be equal to the ratio within the particles. However, this is a poor substitute for a direct measurement of these properties since other things such as particle fracture might inadvertently be included in this calculation and would grossly distort the value, i.e. the value obtained could be partially artifactitious.

A criterion for ductile extension

It is necesary that specific combinations of the mechanical properties of the particles meet one or more criteria for the ductile mechanism of bonding to occur. These were derived in the theoretical paper. One of these can be used to eliminate this mechanism in certain cases, viz. inequality 20 of that paper which is:

$$R < \frac{64 H_0 \Delta\gamma}{3\pi^2 \epsilon_t \epsilon_0 H_t^2}$$

where R is the harmonic mean of the radius of curvature of the surfaces in contact after compression-decompression. The smallest radius of curvature will be assumed to be the particle radius.

When the two particles are of the same size, $R = r/2$ and:

$$r/2 < \frac{64 H_0 \Delta\gamma}{3\pi^2 \epsilon_t \epsilon_0 H_t^2} \tag{9}$$

Also it was deduced that $\epsilon_t/\epsilon_\infty$ must be less than 2 for ductile extension to occur (from part I, Eqn 17). The radius of curvature will increase when the surfaces are deformed plastically during compression. Thus, even if ductile extension occurs (in tension) at low pressures of compression, probably the radius of curvature would become large enough at some compression force for transition to the brittle mechanism to prevail. The criterion derived from this is based on f_c, the compression force acting between two particles. Inequality 18 of part I is:

$$f_c < \frac{256 H_c}{\pi} \left(\frac{\epsilon_\infty H_0 \Delta\gamma}{\epsilon_t \epsilon_0 H_t^2} \right)^2 \tag{10}$$

This criterion suggests that there is always a low enough compression force for ductile extension to occur. However, inequality 9 must be met, also.

Experimental Procedures

General conditions of the tests

To provide an experimental check of this model, it was necessary to obtain estimates of the various parameters for the particles. Since the particles are so small, these had to be derived from measurements made on the compacts. In principle the indentation hardness process has much in common with the compression of particles; a feature in its favor for use in obtaining values for the equations for bonding. Some complications resulted from the fact that the various strain rates used in processing and testing were not known precisely and because the measurement techniques used often did not apply the same strain rate to the entire sample. Consequently, the values used herein are estimates. Nevertheless, the data obtained provide sufficient evidence for the validity of both the brittle and the ductile mechanisms to indicate that additional consideration should be given to these mechanisms.

The experimental procedures used by the authors did not provide all of the information desired. They were those described for determining the tableting indices (Hiestand and Smith, 1984). The first step is to make flawless compacts of the materials being studied. The special triaxial decompression press used to prepare test specimens for the indices determinations was used to prepare the compacts used for these studies. The requirements were the same; its use reduced the probability of hidden fracture regions distorting the experimental results.

Determination of hardnesses and strain index

In the author's laboratory, two indentation hardness apparatuses have been built. Compacts with different solid fractions are used for the determination of the indentation hardness associated with different dwell times. Dwell time is defined as the contact time of the indenter with the surface being indented. The first apparatus is the dynamic, impact indentation hardness apparatus used with the tableting indices measurements (Hiestand et al., 1981, 1984). This is used to provide the best estimate of H_{0c} and ϵ_{0c}. The subscript 0 refers to the impact value, i.e. a dwell time less than 1 ms; and the second subscript, c, is added to indicate that it is the properties of the compact that are being determined. The second apparatus is a motorized screw arrangement that pushes and holds a sphere at a fixed displacement into the tablet. (This apparatus also is used in the determination of tableting indices to meet the need for longer dwell time indentation hardnesses.) The original article (Hiestand and Smith, 1984) defines the bonding index as σ_T/H_{0c}. This is now called the worst case bonding index. (σ_T/H_{tc} where t is 30 min is called the best bonding index.) This permits a displacement to be held constant for a selected interval. It may be used to estimate hardness for various dwell times, i.e. H_t for dwell time, $t > 0$. (The lower limit of dwell time for this apparatus exists since the dwell time should be much longer than the time used to push the sphere into and retract it from the compact.) For this work, the dwell time for the data used was one and one half minutes, the same as the dwell time used for the compression of the com-

pacts.

The radius of curvature of the unloaded dent was used in the estimation of the chordal radius of the dent. A surface analyzer (more commonly used to determine surface roughness) was used for this (Surfanalyzer System 2000, Federal Products Corporation; Providence, RI). The probe in contact with the compact had a spherical end whose diameter was 0.79 mm. The method applied yielded a slightly smaller chordal radius and therefore higher hardness than was obtained with the microscopic estimate of dent size. The impact of systematic errors in determining dent size was minimized in this study because of ratios where systematic errors are at least in part cancelled.

The chordal radius of the dent had not changed significantly with the relaxation of stress after the compact was removed from the indenter apparatus and before the size determination. However, the radius of curvature of the dent would change during this interval. Two different forms of Hertz' laws for spherical surfaces could be obtained to estimate the strain index for different dwell times if the radius of curvature could be determined. However, the time involved in obtaining the radius of curvature caused the procedure to fail. Thus, a simple method for the direct determination of the strain index ratio, $\epsilon_t/\epsilon_\infty$, was not available. When Eqn 8 could not be used as a substitute, it was assumed that the error would be minimal if $\epsilon_t/\epsilon_\infty$ was ignored, i.e. the ratio was taken to be unity.

The dynamic indentation hardness used a steel sphere suspended as a pendulum to strike a tablet. The initial height, h_i, the rebound height, h_r, and the chordal radius of the dent, a, were used in the calculations of the hardness and of the strain index as in Eqns 11 and 12. Most of the equations in the following section apply to the compacts, not the individual particles; the particles are so small they cannot be measured easily.

$$H_{0c} = \frac{4mgrh_r}{\pi a^4}\left(\frac{h_i}{h_r} - \frac{3}{8}\right) \tag{11}$$

$$\epsilon_{0c} = \frac{5a}{6\pi r}\left(\frac{1}{\frac{h_i}{h_r} - \frac{3}{8}}\right) \tag{12}$$

where m is the mass of the indenter, g is the gravitational constant, and r is the radius of the indenter (Tabor, 1951; Hiestand et al., 1971). The measured properties are those of the compact of a given solid fraction. Because the elastic modulus for steel is much larger than that of the compact, it is assumed that that term is negligible in the E' estimate. Thus, the ϵ_0 used in the tablet bond equations is two times the extrapolated value from Eqn 12, i.e. those values reported in Table 2 for particle-particle interactions are twice those obtained with the compact-steel measurement.

To use the model to estimate tablet bond, the properties of the particles are needed. The hardness of the nonporous solid was estimated by using the Leuenberger equation to 'extrapolate' to a solid fraction of one. This was defined as H_0, the maximum value that H_{0c} would have; it is believed to have provided an estimate of the hardness of the solid particles and was obtained using Eqn 13 and nonlinear curve fitting (Leuenberger et al. 1981).

$$H_{0c} = H_0(1 - \exp(-y\sigma_c\rho_r)) \tag{13}$$

where y is a fitting parameter (a compressibility parameter), σ_c is the compression pressure used to make the compact, and ρ_r is the solid fraction (1 − porosity).

The instantaneous strain index values, ϵ_{0c}, were studied as a function of the solid fraction, ρ_r, of the compact (Hiestand and Smith, 1984). Log ϵ_{0c} vs ρ_r was observed to be nearly linear. If curvature developed, it started above a solid fraction of 0.95; and in all such cases it indicated that H_{0c} was increasing more rapidly than E'_{0c} as the solid fraction approached unity. Several studies have indicated that at higher solid fraction, the elastic modulus would increase essentially linearly with solid fraction (Wachtman, 1969). Since over much of the range it was log H that was increasing linearly, the observations are compatible. For lack of specific data, it was arbitrarily assumed that the extrapolation of the log ϵ_{0c} vs ρ_r to solid fraction of one was an adequate estimate of ϵ_0.

Tensile strength measurements

The experimental procedure used for the tensile strength measurements was that previously de-

scribed for the tableting indices measurements (Hiestand and Smith, 1984). With it, the strain rate for a given material is adjusted to at least in part compensate for the effects of viscoelasticity on the test. This may affect the slopes of tensile strength vs N' plots. However, the strain rate at the particle is dependent on the porosity for a fixed platen displacement rate. In the absence of a completely rational method for the selection of a strain rate, the procedures used for the indices were accepted as adequate. Thus, data already obtained for other purposes could be used in this study.

Unfortunately, some other aspects of the tensile strength measurement are arbitrary. Compacts are Mohr bodies; and therefore, the experimental strength depends on the choice of the test conditions, i.e. on the hydrostatic stress at the time of fracture. Also, the reproducibility of the experimental results may be a problem. The procedure used herein with square specimens has numerous advantages: (1) Only a small volume of the central portion of the compact is subjected to the maximum stress; therefore, more consistent results are readily obtained; and (2) An essentially flawless test specimen can be made by compression as in tableting. While the absolute value of its strength may be difficult to predict, the change of strength with solid fraction is relatively easy to observe.

Determining the compression pressure

The ram on the tablet press includes a transducer that provided the total compression force. The compacts used were a 19.05 mm. square with a thickness of about 9.5 mm. Surprisingly the compression pressure values were less reproducible than expected. The σ_c data at high solid fractions seemed to include a very high hydrostatic component. For this reason some of the highest compression data were eliminated. When done carefully, this does not distort the testing of the equations because these occurred far above the transition region. The problem with the hydrostatic stress component in the compression pressure arises because that portion of it that also is hydrostatic stress within the individual particles does not contribute to the increase of the solid fraction. Possibly it would be better to use the hardness value of the compact instead of the actual compression pressure. (This is a part of the reason for the definition of the bonding index being based on hardness instead of compression pressure.)

Choice of particle size

The choice of the particle size to use in the equations has been difficult. Clearly the particle size distribution will influence the results. However, to include the influence of the particle size distribution would complicate the equations excessively. Therefore, a single, mean size was chosen; and in the following calculations, a microscopic evaluation was used. Even this is questionable. For example, with spray dried lactose the particle sizes observed were of aggregates. Probably, these were broken during compression. The Handbook of Pharmaceutical Excipients (1986) lists for spray dried lactose values ranging from < 53 to > 212 μm. It is not unreasonable to assume that most of the particles are aggregates and would fracture. Therefore, the best choice for the particle size would be in the lower range. Microscopic observations confirmed the general conclusion. Microscopic observations of microcrystalline cellulose (Avicel PH-101) showed the particles to be of complex structure. These too probably produced multiple particles of unknown magnitude. Based on microscopic observations, the particle size radiuses used were for spray dried lactose, 25 μm; cellulose, 25 μm; sorbitol, 18 μm; phenacetin, 10 μm; and acetaminophen, 15 μm.

Estimates of the surface energies

The surface energy of a solid is not easy to determine. (Since the examples used herein are self-adhesion cases, $\Delta\gamma$ used in the equations will be twice the values assigned to a single surface.) Techniques using contact angles etc. have been used successfully for low energy solids. However, carbohydrates present a much more difficult problem and errors of measurement are very difficult to avoid. In the following calculations the surface energies were an unknown and the numbers used were either literature values or reasoned estimates. The latter selection was made by assuming that the surface energy of carbohydrates should be

similar to that of glycerol if corrected for specific gravity differences. Ideally one should use the differences of surface densities; but these are unknown. When the cohesive energy density, $\Delta E/V$ (square of the solubility parameter), is known, the relationship between density and surface energy has been determined (Beerbower, 1971). The density to the 2/3 power is one of the factors. Of course, this too is the correction applied when going from volume to surface, i.e. the 2/3 power. Thus, for use here the ratio of densities to the 2/3 power was used for estimating the surface energy.

Glycerol has a specific gravity of 1.29 and a surface energy of 63.4 erg/cm^2. Since the density of a particle of spray dried lactose is 1.53, the surface energy for lactose was taken as 63.3 $(1.53/1.29)^{2/3} = 71$. This is in accord with a literature value (Lerk et al., 1976) for lactose, 71.6. Literature values (Lee and Luner, 1972) for microcrystalline cellulose from contact angles range

TABLE 1

Regression lines obtained for the various compact parameters

Material	Parameter	N' range	Slope (kN/cm^2) ($\times 10^2$)	− intercept (kN/cm^2) ($\times 10^2$)	Correlation coefficient (r)
Sorbitol	σ_T	$N' > 1.20$	51.440	55.191	0.9970
		$N' < 1.18$	24.406	22.101	0.9966
	σ_c	$N' > 1.20$	552.33	625.92	0.9574
		$N' < 1.18$	185.05	163.28	0.9950
	σ_T^2/σ_c	$N' > 1.20$	4.6615	4.5638	0.9278
		$N' < 1.18$	3.1087	2.8605	0.9951
Cellulose	σ_T	$N' > 0.80$	91.863	66.437	0.9980
		$N' < 0.72$	20.688	10.099	0.9954
	σ_c	$N' > 0.80$	1088.3	786.58	0.9887
		$N' < 0.72$	317.48	142.57	0.9966
	σ_T^2/σ_c	$N' > 0.80$	7.7659	5.6154	0.9962
		$N' < 0.72$	1.2551	0.63999	0.9916
Lactose	σ_T	all N'	27.488	28.973	0.9565
	σ_c	all N'	3611.4	3697.3	0.9561
	σ_T^2/σ_c	all N'	0.20415	0.21908	0.9526
	σ_T	$N' > 1.26$	45.618	54.376	0.9960
		$N' < 1.26$	11.048	10.554	0.9970
	σ_c	$N' > 1.26$	6010.8	7063.3	0.9896
		$N' < 1.26$	1821.7	1678.5	0.9996
	σ_T^2/σ_c	$N' > 1.26$	0.34274	0.41306	0.9908
		$N' < 1.26$	0.063775	0.062279	0.9908
Acetaminophen	σ_T	all N'	16.325	18.872	0.9930
	σ_c	all N'	7274	8001	0.9539
	σ_T^2/σ_c	all N'	0.024004	0.02639	0.9752
	σ_T	$N' > 1.23$	17.853	20.764	0.9860
		$N' < 1.23$	6.5318	6.7671	0.9978
	σ_c	$N' > 1.23$	10939	12930	0.9800
		$N' < 1.23$	3177.6	3216.7	0.9947
	σ_T^2/σ_c	$N' > 1.23$	0.02887	0.03288	0.9598
	σ_T^2/σ_c	$N' < 1.23$	0.01282	0.013465	0.9938
Phenacetin	σ_T	all N'	9.155	10.834	0.9903
	σ_c	all N'	1995.0	2318.9	0.9704
	σ_T^2/σ_c	all N'	0.039536	0.046841	0.9722

from 54.2 to 73.9 erg/cm^2. (Different values are obtained with different liquid combinations.) Its density is 1.56; 63.3 $\{1.56/1.29\}^{2/3} = 72$ erg/cm^2. This is close to the upper value reported; and was assumed to be correct. Since sorbitol has the same specific gravity as glycerol, it was assumed to have a surface energy of 63 erg/cm^2.

Acetaminophen would have a significantly lower surface energy. However, a literature value reported for it is 67.7 (Lerk et al., 1976). This seems to the author to be too large a value. There is not a lot of difference between phenacetin and acetaminophen. Two values have been reported for phenacetin, 58.3 (Zografi and Tam, 1976) and 63.1 (Lerk et al., 1976). The author believes both of these to be surprisingly large values, and therefore, used the smaller value. Using the phenacetin for an estimate of acetaminophen, yielded for acetaminophen 58.3 $(1.29/1.24)^{2/3} = 59.9$.

Familiarity with surface energy data instills doubt about any individual value reported; this is supported by the range of values cited for microcrystalline cellulose. Clearly the selection of the value to use for surface energy is at best a judgement influenced by the experience of the specific selector. There will be honest differences of judgement among various workers. This plus other parameters of questionable magnitude make it impossible to obtain a precise check of the equations. However, the potential error from the surface energy is believed to be much smaller than that relating to particle size and perhaps differences in real and assumed strain rates.

Experimental Results

All tensile strength data reported have been plotted against N'. In some cases the plots separate into two sections that appear to be essentially linear. The least square slopes and intercepts are given in Table 1. Fig. 2 shows plots of both σ_T vs N' and σ_c vs N' for sorbitol. The sorbitol data were treated as two intersecting straight lines with a discontinuity in the region of $N' = 1.19$. Fig. 3 shows the same plots for cellulose (Avicel PH-101), Fig. 4 for lactose (spray dried), Fig. 5 for acetaminophen, and Fig. 6 for phenacetin (only one line section). In all cases the transition regions were determined from the tensile strength plots, not the compression pressure plots.

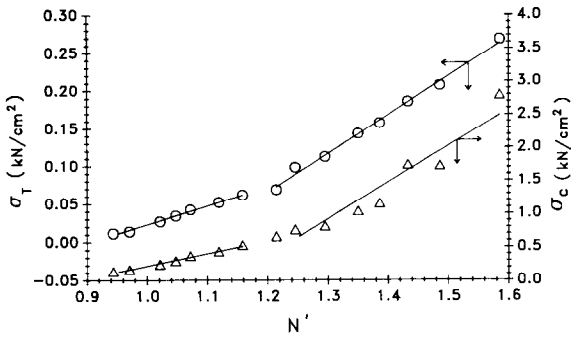

Fig. 2. Sorbitol: plot used to evaluate the ductile mechanism and tablet bond strength. (○) Tensile strength vs N'. (△) Compression pressure vs N'.

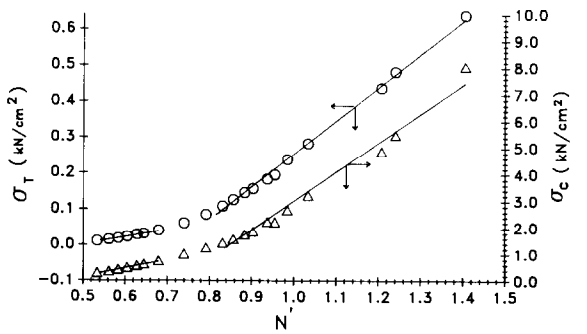

Fig. 3. Cellulose (Avicel PH 101): plot used to evaluate the ductile mechanism and tablet bond strength. (○) Tensile strength vs N'. (△) Compression pressure vs N'.

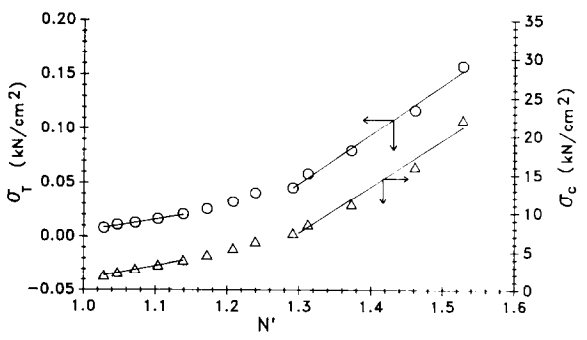

Fig. 4. Lactose (spray dried): plot used to evaluate the ductile mechanism and tablet bond strength. (○) Tensile strength vs N'. (△) Compression pressure vs N'.

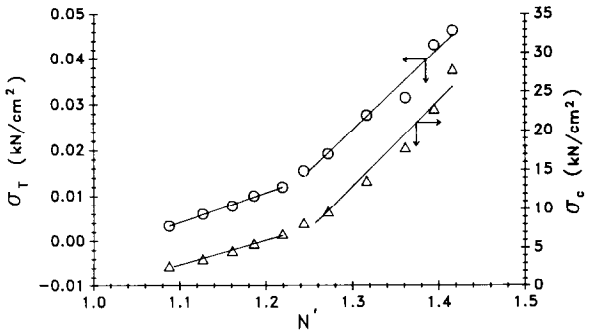

Fig. 5. Acetaminophen: plot used to evaluate the ductile mechanism and tablet bond strength. (○) Tensile strength vs N'. (△) Compression pressure vs N'.

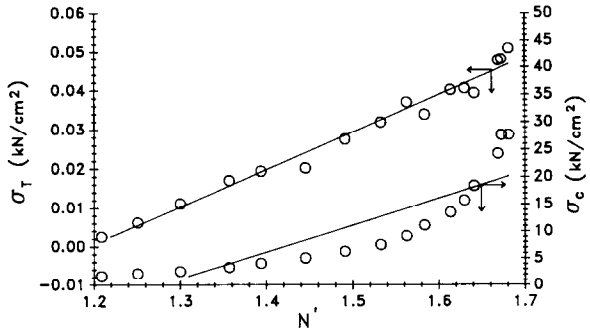

Fig. 6. Phenacetin: plot used to evaluate the ductile mechanism and tablet bond strength. (○) Tensile strength vs N'. (△) Compression pressure vs N'.

These data have provided representation of four very different materials. If isthmus formation is the bonding mechanism, the slopes, k_g', of these lines should correspond to k_p' (Eqn 6). These are tabulated in Table 2. When the brittle mechanism is controlling the bond strength, k_g should correspond to k_p. k_g is obtained from plots of σ_T^2/σ_c vs N', Figs 7–9. The regression line values are given in Table 1; and the calculated and graphical constants are listed in Table 2.

With two linear sections in the plots, the mechanism could be converting from the ductile to the brittle mechanism so that only the upper portion would fit this model. The correlation coefficients obtained with σ_T^2/σ_c plots were less than desired for the reasons mentioned earlier. Also, Table 2 includes the constants calculated for the particle properties and the particle properties on which the constants were based. When data were given for ranges of N', the k_p values in these lines were obtained by using graphical value of $\epsilon_t/\epsilon_\infty$ (Eqn 8). When the k_p value appears in the same line as the hardness data, the k_p value was calculated by assuming the strain index ratio to be one. In this

TABLE 2

Particle properties and comparison of slopes

Material	H_0 (kN/cm²)	ϵ_0 (×10²)	H_t^a (kN/cm²)	$\epsilon_t/\epsilon_\infty$	k_g (×10⁴)	k_p (×10⁴)	k_g' (×10³)	k_p' (×10³)
Sorbitol	64.2	3.36	5.34			150 [b]		
$N' > 1.20$				1.75	466	457	(514) [c]	–
$N' < 1.18$					(311) [c]	–	244	239
Cellulose	20.7	5.76	8.01			1.45 [b]		
$N' > 0.80$				2.45	777	8.43	(919) [c]	–
$N' < 0.70$					(126) [c]	–	207	2.28
Lactose	103.6	4.50	32.5		20.4	0.633 [b]	(275)	1.1
$N' > 1.26$				0.706	34.3	0.316	(456) [c]	–
$N' < 1.16$					(6.38) [c]	–	110	1.01
Aceta-	10.2	4.60	4.99		2.40	3.22 [b]	(132) [c]	5.16
minophen				(0.863) [d]		2.40		
$N' > 1.23$				0.266	2.89	0.228	(179) [c]	–
$N' < 1.23$					(1.28) [c]		65.3	5.16
Phenacetin	8.79	3.04	5.95		3.95	6.87	(91.5)	11.0
				(0.758) [d]		3.95		

[a] Data are for a dwell time of 1.5 min.
[b] $\epsilon_t/\epsilon_\infty$ assumed to be unity to obtain this k_p.
[c] Apparent values; but based on data in area of opposite mechanism.
[d] $(k_g/k_p)^{1/2}$; (needed to make $k_p = k_g$).

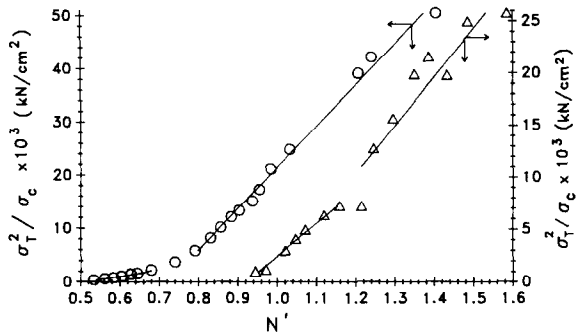

Fig. 7. Cellulose and sorbitol: plot used to evaluate the brittle mechanism and tablet bond strength. (○) Sorbitol. (△) Cellulose (Avicel PH-101).

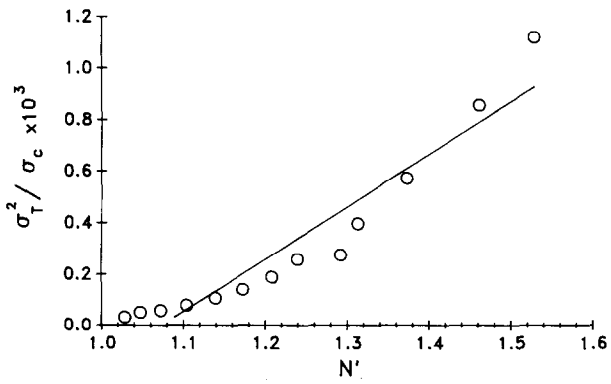

Fig. 8. Lactose (spray dried): plot used to evaluate the brittle mechanism and tablet bond strength.

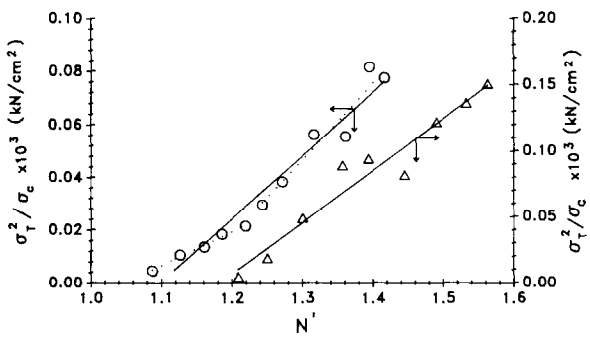

Fig. 9. Acetaminophen and phenacetin: plot used to evaluate the brittle mechanism and tablet bond strength. (○) Acetaminophen: (———) data treated as one line segment; (· · · · · ·) data treated as two line segments. (△) Phenacetin.

case, it will be one sixteenth the value of k_p' as required by the definition of the constants. Even when the tensile strength data yield only one line, both k_g and k_g' are listed even though both cannot be valid in the same portion of the curve. In these cases the brittle mechanism is assumed and the k_p' value is listed but in parentheses. Initially, they are needed for comparison to determine which of the mechanisms is acting, i.e. for determining which of the calculated and graphical values are of similar magnitude.

Discussion

Comparison of slopes to respective particle based constants

Only when two regions, one for each the ductile and the brittle mechanisms, exist, is it possible to determine graphical values for both slopes, k_g' and k_g. These then are used in Eqn 8 to obtain estimates of $\epsilon_t/\epsilon_\infty$, which is used in Eqn 5 to calculate k_p. (Since this graphical method forces the ratio k_p/k_p' to be the same as k_g/k_g', an independent method for estimating the strain index ratio is needed.) It is necessary to recognize the potential risk with this procedure of making an unjustified, artificial adjustment to the magnitude of k_p. However, if the particle properties predict k_g', the theoretical aspects of Eqn 2 are supported. If this is followed by also predicting k_g when applying a reasonable, graphical value for the strain index ratio, the theory receives further support.

For sorbitol k_p' is very close to k_g'. k_p includes the ratio $\epsilon_t/\epsilon_\infty$, which has not been determined; however, the value for this ratio needed to make k_p correspond to k_g is very nearly the same as that calculated using Eqn 8. These values meet the criterion for ductile extension (Part I, Eqn 17). Fig. 2 shows the tensile strength and the compression pressure plots. Inequality 9 would predict that ductile extension would occur for sorbitol as long as the radius, $r/2$, is less than $1.82/\epsilon_t$ μm. Since ϵ_t is expected to be less than 0.04, the criterion for ductile extension is for the particle radius to be about 90 μm. Clearly the first part of the tensile curve fits the ductile model and the second part the brittle model (see Fig. 7). The equations adequately describe the bonding.

For the cellulose, the graphical estimate of $\epsilon_t/\epsilon_\infty$ exceeds 2 (from slopes in Figs 3 and 7); this

suggests that the material would not undergo ductile extension. However, if particles fracture at higher compression pressure, k_g would be increased relative to k_g'. This could cause an incorrect, high graphical value for $\epsilon_t/\epsilon_\infty$. The low hardness value, H_0, would not lead one to expect particle fracture. However, this material is not a well defined crystalline one. Thus, unexpected effects could occur. The particle size criterion would be $0.211/\epsilon_t$ μm. Again assuming that $\epsilon_t < 0.04$, this gives approx. 10.5 μm. If the aggregate fractures into small particles, this criterion would be met. In fact with a mean size of 25 μm, it is possible that there are small enough particles present even before fracture for this criterion to be met. However, if ductile extension occurs, it should convert to the brittle mechanism at a lower value of N' than for sorbitol. The apparent transition for avicel is at about $N' = 0.8$ and for sorbitol at $N' = 1.2$. Thus, it may be reasonable to assume that the ductile extension occurs when N' is low. Clearly, the particle size would have to be much smaller than the 25 μm used to calculate k_p' for it to equal k_g'; 2.6 μm would bring them into correspondence.

The criterion for the radius of curvature for spray dried lactose is $R < 0.067/\epsilon_t$. Again assuming that ϵ_t is less than 0.04, the criterion for particle size is approx. 3.3 μm. While 25 μm was used for the particle size when calculating k_p and k_p', it is known that these particles are aggregates. However, it would be necessary for them to break into more than 13 particles to reach the point where ductile extension would be expected. (13 particles represents a central sphere with a coordination number of 12.) When treating the data as a single line, i.e. ignoring the apparent inflection, one does not have an estimate for k_g'. (The data in Table 2 in the same line as the name of the compound are written assuming that the brittle mechanism is controlling. Thus k_g', 0.275, is put in parentheses.) One cannot estimate $\epsilon_t/\epsilon_\infty$ without having both graphical values. Of course empirical values for particle size and $\epsilon_t/\epsilon_\infty$ can be used to bring correspondence of k_p with k_g and k_p' with k_g'. For example, since $k_g/k_p = 32.2$, $(25\ \epsilon_t/r\epsilon_\infty)^2$ must equal 32.2 to make $k_p = k_g$. If $\epsilon_t/\epsilon_\infty = 1$ and $r = 4.4$ μm, then k_p would equal k_g.

The plots, Figs 4 and 8, indicate that one should explore the possibility that the two sections of the lactose plots arise from an initial ductile region converting to a brittle region. The assumption that both mechanisms occur does not change the radius of curvature criterion. The graphical estimate of $\epsilon_t/\epsilon_\infty$ yields 0.706; relatively low but an acceptable value for ductile extension to occur. The data listed in Table 2 under the two ranges of N' indicate that k_p and k_p' can be made to match the graphical values only by making the particle size become small, 2.4 μm. Again without an independent determination of $\epsilon_t/\epsilon_\infty$ one cannot determine which mechanism is acting. However, the graphical data clearly break into two sections. Thus, it is assumed that ductile extension occurs at the lower compression forces.

The radius of curvature criterion for acetaminophen gives $0.192/\epsilon_t$ μm. If ϵ_t is assumed to be less than 0.04, then for ductile extension to occur, r must be less than about 9.6 μm. Probably some particles are present that meet this criterion since the mean size was 15 μm. The plot of σ_T^2/σ_c vs N' (Fig. 9) appears to be in two straight line sections. (The fact that $k_p > k_g$, when $\epsilon_t/\epsilon_\infty$ is assumed to be one, could be because the assumptions are incorrect, e.g. possibly the strain index ratios are less than one or the strain rate is different from the assumed rate.) Treating it as one line gives excellent correspondence if $\epsilon_t/\epsilon_\infty$ is assumed to be 0.663. No particle size adjustment is needed with this assumption.

When the acetaminophen data are treated as two linear sections, one obtains $k_g' = 0.0653$ from Fig. 5 and $k_g = 0.000289$ from Fig. 9. Since k_p' is 0.00516, the particle size would have to be 4.21 μm to bring them together (k_p' was calculated using 15 μm). The ratio of k_g/k_g' would suggest that $\epsilon_t/\epsilon_\infty$ would be 0.266. This is surprisingly low. Combining the 0.266 factor with the particle size of 4.21 μm the graphical and calculated constants become equal.

If one assumes that the brittle mechanism alone is the better choice, the changes of the slope of these plots must be due to effects not included in the simple theory presented here. The need for an independent measure of the strain index ratio is illustrated by this situation. The graphical transi-

tion is at approximately $N' = 1.23$. This is associated with materials that have a relatively large value for the radius of curvature criterion, which is not the case for acetaminophen. Therefore, it is assumed that the brittle mechanism represents the bonding mechanism principally because the particles are not aggregates and the strain index ratio is more acceptable. Clearly this is a choice based on reasonable but soft evidence.

The change of slope feature is not explained by the brittle mechanism. However, the above discussion ignores the problem of producing a good test specimen. The low solid fraction acetaminophen compacts are extremely soft. Making flawless compacts of undiluted acetaminophen to use for the measurements is not an easy task. This is appreciated by anyone who has had experience with tableting this material. Possibly, the lower section slope is influenced by defects in the compacts. Another possibility arises, if the bonding in the region below $N' = 1.2$ is a mixture of the ductile and brittle mechanisms, then the slope at higher values of N' could correspond while no correspondence with k'_p would exist. k'_p cannot be compared to the apparent k'_g, when the latter is dominated by a mixed process region; insufficient purely ductile region exists. The transition would then occur when the sites of ductile extension were depleted. For this the comparison would be between $k_p = 0.000322$ and $k_g = 0.000289$. If $\epsilon_t/\epsilon_\infty = 0.947$, these would be brought together. This mixed mechanism at low solid fraction is an alternate, reasonable explanation but again must be considered as based on soft evidence. Nevertheless, it is the most attractive explanation because of the more reasonable value for the strain index ratio.

With phenacetin, only the brittle mechanism is considered (Fig. 9). The k_g is 0.00395 and k_p is 0.00687 with $\epsilon_t/\epsilon_\infty$ taken as unity. The magnitude of $\epsilon_t/\epsilon_\infty$ would need be only 0.759 to bring the two numbers together. If one considers the assumptions used to estimate k_p, this is a very reasonable correspondence with theory. The brittle mechanism describes the bonding process.

While the correspondence of the calculated and experimental slopes was not as close as desired, the differences appear to be easily explained. Because of the many estimates made to obtain the data, at this point one is limited to saying that the data are not inconsistent with the theoretical model. However for sorbitol, the correspondence was sufficient to add direct support for the theory.

Predicting the transition region

If an apparent transition occurs, the general discontinuity region of the transition can be predicted using the concepts of the theory. In inequality 10, it is expedient to assume that $H_c = H_t$. Multiplying the left side by N yields σ_c (f_c is assumed to be the mean value, f_{cm}) and the right side by N'/r^2, the equivalent of N, and then substituting k_p or k'_p for the equivalent terms, one obtains inequality 14.

$$\frac{\sigma_c}{N'} < 64k_p\left(\frac{\epsilon_\infty}{\epsilon_t}\right)^4 = 4k'_p\left(\frac{\epsilon_\infty}{\epsilon_t}\right)^2 \tag{14}$$

If there is a transition from the ductile mechanism to the brittle mechanism, it should be in the region where the two sides of inequality 14 are equal as in Eqn 15.

$$\left.\frac{\sigma_c}{N'}\right|_d = 64k_p\left(\frac{\epsilon_\infty}{\epsilon_t}\right)^4 = 4k'_p\left(\frac{\epsilon_\infty}{\epsilon_t}\right)^2 \tag{15}$$

Intuitively, one may feel that the intersection of the two lines of the tensile strength vs N' plot is a clear indication of the transition point. However, if ductile extension does occur, the tensile strength-compression pressure relationship between two particles may not be a continuous function. In fact if one assumes that at the transition the strength of an individual contact would be the same for both the ductile and brittle mechanisms, one would obtain (when $H_c = H_t$) a value of f_c equal to four times the magnitude of the upper limit of the criterion of f_c for ductile extension.

For an individual contact point the transition from the ductile to the brittle mechanism causes an immediate decrease of tensile strength. However, as f_c is increased further, the strength of the brittle case will soon exceed that of the earlier ductile case. The tensile strength of a compact

does not follow this drop of strength because not all contact points simultaneously reach the critical f_c value. The transition is spread over a significant range of the compression force. At the start of the transition, enough new ductile contacts are established to essentially compensate for the loss of strength of those that become brittle. Clearly, the transition has started at a value significantly lower than the intersection point of the two straight line sections. Thus, the predicted value of N' for the transition should be at a lesser N' value than that at the intersection of the two line segments. Either the brittle or the ductile portions of the σ_c vs N' plot could be used to estimate the N' value at the transition. Because the slope of σ_c vs N' is larger in the brittle region, and because the predicted σ_c/N' will be less than at the intersection of the two lines, the brittle region portion will provide the better estimate of the apparent, graphical transition.

The earlier data indicated that sorbitol underwent ductile extension at lower values of N'. The criteria were met and the correspondence of the constants were good. For sorbitol the transition condition is $\sigma_c/N' = 0.312$ (Eqn 15); Fig. 2 shows a plot of σ_c vs N'. The regression line for the ductile region, $\sigma_c = 1.851\ N' - 1.633$, would yield: $0.312 = 1.851 - 1.633/N'$, $N' = 1.06$. When the regression line for the brittle portion of the curve is used for this calculation, the prediction for the transition would be at $N' = 1.20$; very close to the intersection of the two lines. Both values are below the intersection of the two lines, $N' = 1.22$. This confirms the prediction in the preceding paragraph that the brittle region provides the better estimate.

It is of interest to check other materials. Because of the particle size problem discussed above for microcrystalline cellulose, k_g will be used in place of k_p; $64k_g(\epsilon_\infty/\epsilon_t)^4 = 0.141$. Only the regression line for the brittle region will be used. This yields $N' = 0.73$. Again the brittle region predicts the approximate value for the intersection of the two lines; the graphical value is about $N' = 0.79$.

Spray dried lactose also shows an inflection in the tensile strength and the compression pressure plots. If the transition is accepted, the material would undergo ductile extension at the lower compression forces. With lactose, the intersections of the straight line sections occur at approximately $N' = 1.26$. The curvature extends over a range from N' equals 1.16–1.28. Eqn 15 yields $\sigma_c/N' = 0.893$; which when used in the equation for the regression line predicts $N' = 1.18$. This prediction based on the brittle line is close to the start of the curvature associated with the transition.

All three cases examined have followed the same pattern. It has been shown that Eqn 15 and the regression line for the brittle mechanism region of the tensile strength can be used to calculate the approximate transition region, i.e. the value of N' for the transition from the ductile to the brittle region of the bonding mechanism. Again consistency with the theoretical model is obtained.

The intercepts, b and b'

A hypothetical value of N', for the condition when the tensile strength of the compact became essentially zero, N_0', might be deduced from modeling the structure of powder beds. With powders, the contact areas resulting from the molecular forces acting between contacting particles produces a contact area larger than the critical value for the brittle mechanism (Hiestand, 1991). Thus strength is present as long as there is continuity from particle to particle. Again one must recognize that the equations used for calculating N' are valid only after the structure has developed to a significant degree. In the very early stages of consolidation, the development of strength cannot be measured by the techniques described herein. Since the powder bed has only a weak strength, the value for N_0' should be very nearly the same for both tensile strength and for compression pressure. It is interesting to examine the experimental cases.

For the ductile region of sorbitol, the tensile strength plot (Fig. 2) extrapolates to $N_0' = 0.86$ and the compression pressure to $N_0' = 0.88$. The brittle regions extrapolate to $N_0' = 1.06$ and 1.10, respectively. These are surprisingly close to expectations. The same comparison of N_0' values for cellulose gives for the ductile region values of $N_0' = 0.49$ for the tensile strength and $N_0' = 0.45$ for the compression pressure. The brittle region

plots both extrapolate to $N_0' = 0.72$. Clearly the value of N', where the tensile strength becomes very small, is different for different materials.

In the absence of better data, a good estimate of the intercept of the tensile strength plots is obtained by assuming that the N_0' value is the same for both compression and tension. b and b' can be estimated from the slopes, k_p and k_p', and the respective N_0' values. The approximate correspondence of the N_0' values for the σ_T vs N' (ductile mechanism) and the σ_c vs N' plots suggests that the state of consolidation at which these stresses become significant is similar for both. The interdependence of the tensile strength and compression pressure in the brittle mechanism region is supported by the similarity of the N_0' values in

Glossary

Symbol	Meaning
a	chordal radius of circular contact region between spherical indenter and compact
b	absolute value of intercept for brittle mechanism tensile strength Eqn 3
b'	absolute value of intercept for ductile mechanism tensile strength Eqn 4
d	subscript in Eqn 15 to show evaluation is at ductile limit
E	Young's Modulus of elasticity, subscripts identify particle 1 or particle 2
E'	complex elastic modulus, two materials; see Eqn 1
E_{0c}'	complex elastic modulus of compact, instantaneous
f_{am}''	mean pull off force for spherical surfaces; brittle mechanism, viscoelastic material
f_{adm}	mean pull off force for spherical surfaces; ductile extension of surfaces
f_c	compression force for spherical surfaces
f_{cm}	mean compression force per particle
h_i	initial height of indenter for impact indentation
h_r	rebound height of indenter after impact
H	indentation hardnesses of the particle
H_0, H_t, H_∞	indentation hardnesses of particles, subscripts refer to strain rates, 0 is instantaneous, t for time t, and ∞ for totally relaxed
H_c	indentation hardness of particles at strain rate used for the compression of the compact
H_{0c}	indentation hardness of the compact, instantaneous
H_{tc}	indentation hardness of compact with strain rate resulting from strain rate associated with time t
k_g	slope, equivalent to k_p but obtained from graphical data
k_p	tensile strength parameter for the ductile process that is calculated from the particle properties (Eqn 5)
k_g'	slope, equivalent to k_p' but obtained from graphical data
k_p'	tensile strength parameter for the brittle mechanism that is calculated from the particle properties (Eqn 6)
m	mass of the spherical indenter used in impact hardness
N	the number of interparticle contacts in a cross section of the compact that must be separated during fracture
N'	Nr^2; number of contacts in an area r^2 separated by fracture
N_0'	the value of N' obtained by extrapolating to zero tensile strength
r	the radius of the individual particles or indenter
R	the harmonic mean of the two contacting spherical surfaces
γ	compressibility parameter in Eqn 13
$\Delta\gamma$	change of surface energy going from free surface to solid solid interface
ϵ	H/E'; the strain index, relative strain at spherical surfaces following plastic deformation during compression
ϵ_0, ϵ_t, ϵ_∞, ϵ_c	subscripts refer to strain rate as in definitions of H
ϵ_{0c}	strain index of the compact, instantaneous
υ	Poisson's ratio, number subscripts refer to particle 1 or particle 2
ρ_r	relative density, solid fraction, volume fraction of solid of the compact
σ_c	maximum compression stress on the compact when making it
σ_T	tensile strength of the compact; brittle mechanism
σ_{Tv}	compact tensile strength; brittle mechanism, viscoelastic material
σ_{Td}	compact tensile strength; ductile mechanism

this region. Since this interdependence is predicted by the model the success is support for the validity of the model.

Slope of the compression pressure vs N' plot

It is obvious by examining Eqn 1 that the compression pressure vs N' plot is related to the tensile strength plot, i.e. σ_T is proportional to $\sigma_c^{1/2}$ when the bonding is the brittle mechanism. This is not true for Eqn 2 where bonding is controlled by the ductile mechanism. In the ductile region both σ_T and σ_c are directly proportional to N'. The slope of the σ_c vs N' plot is f_{cm}/r^2 when both f_{cm} and r are constant. While N' is increasing as the compression pressure increases, f_{cm} may not increase since it is a mean value. New contact points start at very small values of f_c. This is supported by the fact that often the σ_c vs N' plot is essentially linear in this region. Therefore, in the ductile mechanism region, the slopes of both the compression pressure plot and the tensile strength plots essentially are directly proportional to N'. A plot of σ_T vs σ_c should have a slope equal to $k'_p r^2/f_{cm}$ in the ductile region.

This suggests further speculation. Probably f_{cm} could remain roughly constant only as long as the consolidation mechanism involves significant particle rearrangement. The f_c acting on any one particle would be limited because of the particles sliding over each other. However, once the consolidation reaches a point where particle rearrangement is very inhibited, the average force at each individual contact will start to increase rapidly. Thus, it exceeds the criterion of inequality 10 and the mechanism of bonding changes. The change away from particle rearrangement could lead to a change in the slope of the compression pressure plot. Thus, the approximate correlation of the transition regions may be real, both occurring because the f_{cm} started to increase rapidly as the mechanism of consolidation changed.

Conclusions

Two different mathematical models, two different mechanisms, of tablet bond formation have been tested against experimental data. For well defined crystalline materials, the equations provided very good results if allowance was made for the many estimates that went into the calculations. Only an average particle size was used even though particle size distribution and particle shape could be important. The equations provided a criterion for the potential conversion from one mechanism to the other as the solid fraction increased. When directly measured data for the properties of compacts were used, the theory provided the equations to predict at what solid fraction the transition would occur. These results have supported the general tenets of the theory. Obviously, much more must be done to obtain the needed particle data for a thorough testing of the theoretical models.

References

Beerbower, A., Surface free energy: a new relationsip to bulk energies. *J. Colloid Interface Sci.*, 35 (1971) 126–132.

Handbook of Pharmaceutical Excipients, American Pharmaceutical Association, Washington, DC, 1986.

Hiestand, E.N., Tablet bond. I. A theoretical model. *Int. J. Pharm.*, 67 (1991) 217–229.

Hiestand, E.N., Bane Jr, J.M. and Strzelinski, E.P., Impact test for hardness of compressed powder compacts. *J. Pharm. Sci.*, 60 (1971) 758–763.

Hiestand, E.N. and Smith, D.P., Indices of tableting performance. *Powder Technol.*, 38 (1984) 145–159.

Johnson, K.L., Adhesion at the contact of solids. In Koiter, W.T. (Ed.), *Theoretical and Applied Mechanics*, North Holland, Amsterdam, 1976, pp. 133–143.

Lee, S.B. and Luner, P., The wetting and interfacial properties of lignin. *Tappi*, 55 (1972) 116–121.

Lerk, C., Schoonen, A. and Fell, J., Contact angles and wetting of pharmaceutical powders. *J. Pharm. Sci.*, 65 (1976) 843–847.

Leuenberger, H., Hiestand, E. and Sucker, H., Ein Beitrag Zur Theorie der Pulverkompression. *Chem. Ing. Tech.*, 53 (1981) 45–47.

Rumpf, H., The strength of granules and agglomerates. In Knepper, W.A. (Ed.), *Agglomeration*, Interscience, New York, 1962, pp. 379–418.

Tabor, D., *The Hardness of Metals*, Oxford University Press, Amen House, London, 1951.

Wachtman, Jr, J.B., Elastic deformation of ceramics and other refractory materials. In Wachtman, Jr, J.B. (Ed.), *Mechanical and Thermal Properties of Ceramics*, NBS Special Publication 303, NBS, Washington, DC 1969, pp. 139–168.

Williams, J.G., *Stress Analysis of Polymers*, 2nd Edn, Ellis Horwood, Chichester, 1980. p. 124.

Zografi, G. and Tam, S., Wettability of pharmaceutical solids: estimates of solid surface polarity. *J. Pharm. Sci.*, 65 (1976) 1145–1149.